

Multi-parameter study of CO₂ electrochemical reduction from concentrated bicarbonate feed

Carlos Larrea^{*}, Daniel Torres, Juan Ramón Avilés-Moreno, Pilar Ocón

Universidad Autónoma de Madrid (UAM), Departamento de Química Física Aplicada, C/Francisco Tomás y Valiente 7, 28049, Madrid, Spain

ARTICLE INFO

Keywords:

Bicarbonate electrochemical reduction
CO₂ electrolysis
Carbon capture and utilization
Syngas production

ABSTRACT

The electrochemical reduction of CO₂ (CO₂RR) from a concentrated (bi)carbonate solution represents a novel approach of supplying carbon feedstock to a reactor. While this approach achieves comparable performance to gas-feed systems, it substantially reduces the amount of residual CO₂ in the output, simplifying the separation of reduction products from unreacted CO₂. In this work, the reduction of CO₂ to CO from a 2 M KHCO₃ solution will be studied by determining the influence of the membrane's polarity, anolyte's pH and temperature on CO₂RR in a zero-gap flow cell. These parameters were evaluated by measuring the cell potential, the faradaic efficiency (FE_{CO}) and residual CO₂ at current densities (*J*) between 25 and 200 mA cm⁻². The results obtained show that bipolar membranes offer a much higher FE_{CO} compared to cationic or anionic membranes (~45 % to ~12 % at 200 mA cm⁻² at 50 °C) thanks to their ability to dissociate water and produce H⁺ towards the cathode. However, bipolar membranes exhibit an important drawback in the form of a higher cell potential, and higher residual CO₂. The anolyte doesn't affect FE_{CO} significantly when the pH stays within an alkaline value. Also, it was confirmed that higher temperatures improve the FE_{CO} (especially at higher current densities) while reducing the cell potential. Finally, it was determined that the residual CO₂ in the output gas composition stays within 20 %–55 % (at *J* ≥ 100 mA cm⁻²), well below the 60–95 % range obtained in systems with gaseous CO₂ feed, demonstrating the benefits of working with a bi(carbonate) feed.

1. Introduction

Carbon dioxide (CO₂) emissions generated by the combustion of fossil fuels and other anthropogenic activities has driven CO₂ concentration in the atmosphere to reach its high levels in human history [1,2]. The increase in atmospheric CO₂ is the main cause of rising global temperatures, triggering climate change and posing a significant threat to society [3]. This has prompted the search for innovative techniques for recycling CO₂ emissions through Carbon Capture and Utilization (CCU) technologies [4].

The electrochemical reduction reaction of CO₂ (CO₂RR, Eq. 1) offers a potentially scalable method for transforming this molecule into value-added chemicals and fuels. Specifically, CO₂ can be electrochemically reduced to carbon monoxide (CO), a major component -along with H₂- of syngas which is the main precursor of methanol [5] or can be turned into long-chain hydrocarbons through the Fischer-Tropsch (FT) process [6]. This process enables the storage of renewable electrical energy as chemical energy and promotes a diminishing dependence on fossil fuels.

For CO₂RR to become industrially relevant, the technology must

reach milestones across 5 different performance metrics (Fig. 1). It is important to remember that these 5 metrics are interlinked and that adjusting one of them will cause the rest to be altered. The first metric is the *faradaic efficiency* (FE) which describes the catalyst's ability to reduce CO₂ selectively. The FE_{CO} is defined as the amount of electrical charge used to reduce CO₂ towards CO instead of other CO₂RR products or to H₂ through the competitive hydrogen evolution reaction (HER, Eq. 2a-b). Silver and gold catalyst tend to have high FE_{CO} and produce only CO and H₂ as gaseous products in aqueous systems [7]. A minimum FE_{CO} of 33 % is required to obtain a syngas mixture with molar relation CO:H₂ of 2:1. This ratio is needed for syngas to be used in methanol synthesis or FT process [8]. However, a higher FE_{CO} and closer to 100 % is preferred since the H₂ needed for the syngas mixture can be obtained much more energy-efficiently from commercial alkaline or PEM electrolyzers [9]. The second metric is the *current density* (*J*), defined as the current applied to the reactor divided by the area of the electrode, and it is directly related to the rate of production of CO and H₂. A current density higher than 200 mA cm⁻² is considered necessary for an industrial electrochemical process [10]. Usually, when CO₂ electrolyzers operate

^{*} Corresponding author.

E-mail address: carlos.larrea@uam.es (C. Larrea).

<https://doi.org/10.1016/j.jcou.2021.101878>

Received 1 October 2021; Received in revised form 17 December 2021; Accepted 25 December 2021

Available online 10 January 2022

2212-9820/© 2021 The Author(s).

Published by Elsevier Ltd.

This is an open access article under the CC BY-NC-ND license

(<http://creativecommons.org/licenses/by-nc-nd/4.0/>).

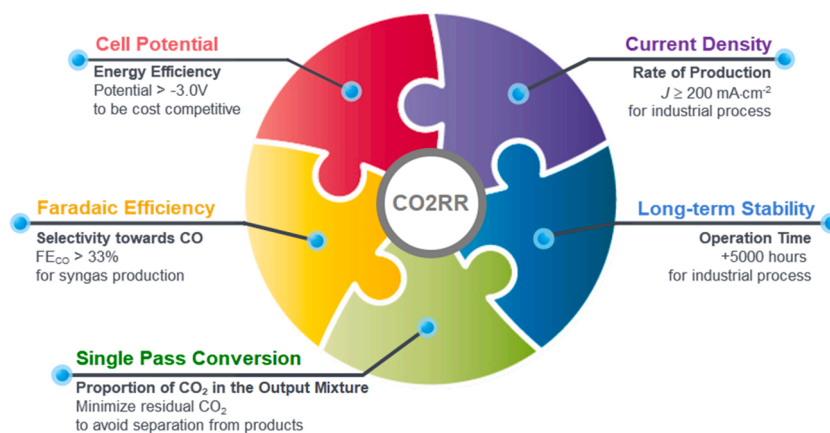
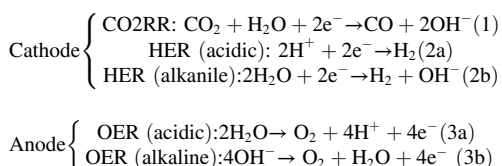


Fig. 1. Performance metrics of CO₂RR systems. Related variables are outlined in bold.

above 100 mA cm⁻², HER starts dominating causing a decrease in FE_{CO} due to mass transport limitation of CO₂ to the cathode. The third metric is the *cell potential*, defined as the voltage maintained by the reactor to enable the flow of a particular current density *J*. The metric is related to the energy efficiency of the electrochemical processes. A cell potential less negative than -3.0 V at current densities in excess of 200 mA cm⁻² and FE_{CO} > 90 % is needed for the CO₂RR process to become cost competitive [11]. The cell potential is comprised of three main contributions: the half-cell potential of the cathodic reactions where CO₂RR and HER occur simultaneously; the half-cell potential of anodic reactions where the oxygen evolution reaction (OER, Eq. 3a-b) takes place in most systems; and the potential drop caused by the membrane's ohmic resistance. The fourth metric is the *stability* of the system which sets out that the electrolyser has to operate at near constant conditions (i.e. cell potential, *J*, and FE_{CO}) for long periods of time. Catalyst deactivation and membrane degradation are some of the causes that affect the stability of a CO₂ electrolyser [10,12]. Currently, there exist CO₂RR systems that can operate for 650 h with high stability [13]. However, Martin et al. consider 5000 h of continuous operation as a figure of merit since PEM electrolyzers can operate continuously beyond 20000 h [14].



The final metric -often overlooked in the literature- is the *single pass conversion* of CO₂ which is calculated by dividing the number of moles of CO₂ transformed into CO by the number of moles of CO₂ introduced to the cell. A low single pass conversion makes it difficult and costly to separate the reduction products from the unreacted CO₂. Another way of evaluating this parameter is by measuring the concentration of CO₂ in the gaseous mixture that comes out of the cell, which in this paper will be called "residual CO₂".

In the last few years, most of the research has focused on developing CO₂ electrolyzers that use a gaseous feed of CO₂ as input. This approach has the advantage of achieving high FE_{CO} at high current densities since it avoids mass transport limitations and suppresses HER [15,16]. However, for this approach to achieve such good results, a large excess of CO₂ is needed as input resulting in a gaseous output mixture composed of >60 % of residual CO₂ [13,17,18]. More recently, in an effort to reduce the amount of residual CO₂, Tengfei Li et al. and Yuguang Li et al. demonstrated the use of purely aqueous catholyte of concentrated carbonate (CO₃²⁻) or bicarbonate (HCO₃⁻) species as a way to supply CO₂ to the cell [19,20]. This novel approach avoids the need of a gaseous CO₂ feed into the reactor and thus lowers the proportion of residual CO₂ in

the output. Both authors used bipolar membranes to enable the in-situ generation of CO₂ inside the electrochemical reactor which would then be transformed into CO by a silver-based cathode. Furthermore, working with a concentrated (bi)carbonate aqueous feed has the additional advantage that it makes the CO₂ electrolyser simpler to integrate to hydroxide-based direct-air capture (DAC) systems [21]. By using the (bi)carbonate solution formed from the capture reaction between CO₂ and hydroxide, it is possible to skip the energy-intensive thermal regeneration step needed to liberate the captured CO₂ in the DAC process.

In CO₂ electrolyzers with (bi)carbonate feed, the electrochemical reduction must be thought of as a process where two competing reactions -CO₂RR and HER- occur simultaneously, and where each of the operational and structural parameters will benefit or hinder one reaction over the other. For CO₂RR to actively compete with HER, a continuous supply of dissolved CO₂ (CO_{2(aq)}) has to be supplied to the cathode for its reduction [22]. In this case, since no gaseous CO₂ is delivered to the system at any stage of the process, the dissolved CO₂ used in the CO₂RR is provided by bicarbonate ions that dissociate to form CO_{2(aq)} through rapid chemical equilibrium [23]. The chemical equilibrium and concentration of the carbonaceous species (CO₂ - HCO₃⁻ - CO₃²⁻) is determined by the pH and temperature of the solution, with near-neutral pH being favorable for the formation of CO_{2(aq)}. Since both CO₂RR and HER have OH⁻ ions as a product, the local pH near the cathode's interface will increase during operation (Fig. 2), causing the chemical equilibrium to shift away from CO_{2(aq)} towards higher concentrations of HCO₃⁻ and CO₃²⁻ ions [24]. Therefore, ion transport through the membrane determined by the membrane's polarity and anolyte solution, as well as local temperature, will play an important role in CO₂RR since these parameters have to ability to regulate the local pH at the cathode's surface during operation. However, it is important to keep in mind that HER still at play and some parameters will promote this reaction more than CO₂RR.

This work will further investigate the CO₂RR process from concentrated bicarbonate electrolyte in a flow cell reactor. It will explore the influence of three structural and operational parameters: membrane polarity, the anolyte's pH, and temperature inside the reactor. The study will provide a detailed exposition of the influence on the performance parameters of FE_{CO}, current density, cell potential, and residual CO₂. Even though there exist some papers that investigate the CO₂RR with bipolar membranes, it is unclear how this membrane's performance compares to common cationic or anionic membranes. In the same way, the residual CO₂ generated hasn't been reported in most of the experimental conditions presented in literature. The influence of the pH of the anolyte will also be studied since it is possible that due its proximity to the cathode in zero-gap cell configuration and the membrane's ion transport, the cathodic reactions can be affected. This work won't look

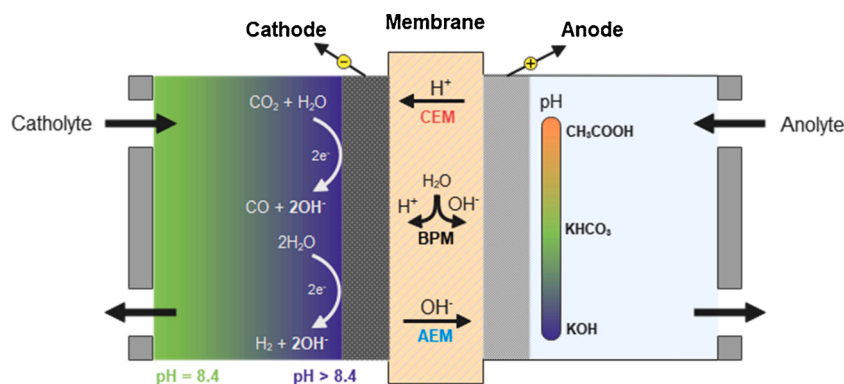


Fig. 2. Flow cell scheme showing the schematic chemical processes involved in the anode, cathode and membranes used in this work.

into the long-term stability of the system due to the scope of the study, but the authors understand its importance and will explore it in future investigations.

2. Experimental methods

2.1. Membrane electrode assembly (MEA)

In this study, unsupported Ag nanoparticles were used as the catalyst in the cathode. The catalyst ink was prepared according to the procedure presented by Verma et al. [15]. The ink was prepared by mixing 42 mg of Ag nanopowder (<100 nm, 99.5 % trace metals basis, Sigma Aldrich), 55 μ L of Nafion solution (5 wt%, Sigma Aldrich), 1600 μ L of deionized water and 1600 μ L of isopropyl alcohol (2-Propanol, LabKem). The mixture was sonicated (Selecta Ultrasons) for 20 min. The ink was then spray-coated onto a GDL of carbon cloth (Fuel Cell Store) with an area of 4 cm² (2 × 2 cm²) until it reached a catalyst loading of 2 mg cm⁻² (\pm 0.1 mg cm⁻²). The catalyst loading was determined by weighting the GDL before and after deposition.

Nickel foam was used as the anode due to its good stability in alkaline conditions, favorable electrocatalytic performance for the oxygen evolution reaction (OER), and relatively low price compared to Ir or Ru based anodes [25]. The area of the anode was of 4 cm² (2 × 2 cm²).

An ion-exchange membrane (3 × 3 cm²) was placed between the cathode and the anode to form the membrane electrode assembly (MEA). Nafion 117 (DuPont), Fumasep FAA-3-30-PE (FuMA-Tech) and Fumasep FBM (FuMA-Tech) were used as the cation exchange membrane (CEM), anion exchange membrane (AEM) and bipolar membrane (BPM), respectively.

A new set of cathode, anode and membrane (MEA) were prepared and used for each experiment with a different membrane/anolyte combination (e.g., one MEA was used for collecting the 3 data points at current densities 25, 50, 100 mA cm⁻² for temperature of 20 °C, and 4 data points at current densities of 25, 50, 100, 200 mA cm⁻² for temperature of 50 °C).

2.2. Electrolytes

The catholyte used for the experiments was a 2 M KHCO₃ solution with 0.02 M of ethylenediaminetetraacetic acid (EDTA, Sigma Aldrich). Potassium was selected as the counter-ion of the bicarbonate salt due to its ability to enhance the selectivity towards CO in Ag catalysts [26]. The concentration of 2 M was selected through preliminary experiments that optimized the FE_{CO} and residual CO₂. While higher concentrations of bicarbonate (>2 M) resulted in slightly better FE_{CO} as observed by Li et al. [20], they also increased the amount of residual CO₂. EDTA was added to the catholyte to remove trace metal ion impurities found in the electrolyte and prevent the deactivation of the catalyst due to their deposition [27].

As for the anolyte, three different solutions were tested in independent experiments to explore the influence of anolyte's pH on CO₂RR. To test a wide range of values in the pH spectrum, the anolytes used were either a solution of 1 M KOH (pH = 14.0), 1 M KHCO₃ (pH ~ 8.4) or 1 M CH₃COOH (pH = 2.4).

2.3. Flow cell reactor setup

The setup of the CO₂ electrolyser system with the reactor and the rest of the components is shown in Fig. 3. The experiments were performed in a two-electrode electrochemical flow cell reactor. The reactor consisted of two compartments separated by the MEA where the catholyte and anolyte flowed. The reactor contains two graphite flow plates pressed together by two current collector plates which act also as housing of the reactor. PTFE gaskets were pressed between the flow plates to have a gas and liquid-tight system. The temperature of the reactor was increased through resistive heating attached to the housing and was regulated using a temperature controller (Eurotherm 2408).

The volumes of catholyte and anolyte were 150 mL and 100 mL, respectively and were held in two separate containers. They flowed through the reactor independently at a rate of 10 mL min⁻¹ using two peristaltic pumps (Dinko Instruments D-25V). Fresh electrolytes were used for each set of experiments.

A phase separator was used to separate the gaseous products formed in the cathode from the aqueous electrolyte. Before the experiments, the volume of the phase separator was completely filled with catholyte before sealing the top of the separator with a rubber stopper, making sure there were no gases present. It was confirmed that only aqueous solutions (i.e. no visible gas bubbles) entered or exited the cell in the cathodic and anodic sides. Gaseous products were formed inside the cell and were carried out by the electrolytes only when electrical current was applied to the reactor during the experiments. The gaseous products that exited the cathodic side of the flow cell were carried by the catholyte and were accumulated in the phase separator. The gaseous products from the anodic side (i.e. O₂) were carried by anolyte and liberated to the atmosphere once they reached the anolyte container.

2.4. Electrochemical measurements and product analysis

Electrochemical measurements were done using a Autolab PGSTAT302N potentiostat/galvanostat. In each experiment, current was applied to the cell up to when the volume of accumulated gaseous products in the phase separator reached 20 mL. Two samples of the gaseous output mixture of 0.5 mL were extracted from the phase separator using a gas syringe. The samples were diluted with 4.5 mL of argon to proceed to the product analysis. These samples were analyzed using a gas chromatographer-mass spectrometer system (GC-MS; GC: Varian 3900 with Carboxen-1006 PLOT Column, MS: Pfeiffer Vacuum Hi-Cube). Argon was used as the carrier gas. The proportions of H₂, CO

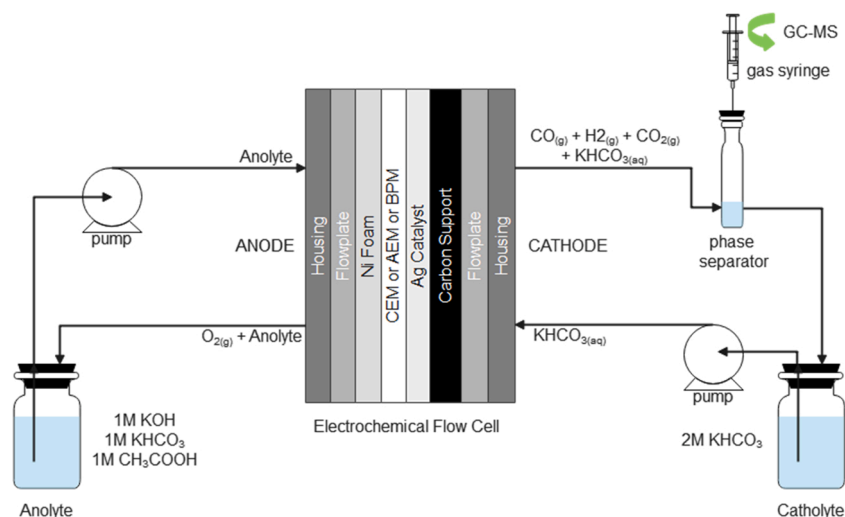


Fig. 3. Experimental set-up of CO₂ electrolyser system.

and CO₂ were quantified using this GC–MS system. No other gaseous products were detected.

The GC–MS was calibrated everyday it was used by analyzing 3 independent 0.5 mL gaseous samples of H₂, CO and CO₂ at 100 % concentration each. The samples were diluted in 4.5 mL of argon using the gas syringe. The gaseous mixtures obtained during the experiments were compared to the calibration points in order to quantify the corresponding proportion of H₂, CO and CO₂ in the mixture. A linear relation between concentration and peak intensity was assumed for the quantification. The linear relationship between the two variables was corroborated on separate tests.

3. Results and discussion

Three types of membranes (CEM, AEM and BPM) were tested with three different anolytes representing a broad spectrum in the pH range: KOH (alkaline), KHCO₃ (quasi-neutral), and CH₃COOH (acidic). For each membrane/anolyte combination, experiments were carried at temperatures of 20 °C and 50 °C. For the experiments at 20 °C, chronopotentiometries were done at current densities of 25, 50 and 100 mA cm⁻², while at 50 °C the current densities were increased up to 200 mA cm⁻² since better results were expected. Cell potential, FE_{CO} and residual CO₂ were measured for each experiment.

The experiments with CH₃COOH as the anolyte gave unanticipated results. In the system with CEM/CH₃COOH, HER was completely favored over CO₂RR, with no presence of CO detected as product at any current density. As for the AEM/CH₃COOH and BPM/CH₃COOH systems, the acid attacked the chemical structure of the membrane causing the system to fail and not being able to generate any products. Therefore, from this point onward, the results that will be presented are from the systems with KOH and KHCO₃ in the anolyte.

3.1. Effect on faradaic efficiency towards CO

The membrane's polarity shows small differences in FE_{CO} when comparing between systems with CEM and AEM, with the former promoting slightly better CO selectivity compared to later. In both cases, the FE_{CO} at all current densities studied stays below 33 %, the threshold needed for a useful syngas mixture (Fig. 4a–d). In zero-gap CO₂ electrolyzers, it is expected that these two types of membranes make use of their ion-exchange capabilities in order to regulate the pH at the cathode's surface. The cationic membrane allows the transport of positive ions (H⁺ and K⁺) from the anode side to the cathode, while the anionic allows the transport of negative ions (OH⁻) from the cathode to the

anode side. Results obtained indicate that ion-transport is insufficient to effectively promote CO₂RR over HER.

On the other hand, the bipolar membrane shows a big improvement in FE_{CO} (Fig. 4e, f) compared to CEM and AEM. Lately, bipolar membranes have become more popular in CO₂RR systems since they inhibit the crossover of neutral species from both sides of a cell and have the ability to dissociate water molecules into H⁺ and OH⁻ [28]. Working under reverse bias, the BPM membrane generates a flow of H⁺ towards the cathode and OH⁻ towards the anode, a property that can regulate the local pH of the cathode more effectively than CEM and AEM membranes which only transport ionic species. This is reflected by a significant increase in selectivity towards CO from ~ 25 % and ~ 10 % with CEM or AEM to ~ 60 % and ~ 30 % with BPM at a current density of 25 and 100 mA cm⁻² respectively.

Concerning the anolyte's pH effect on the faradaic efficiency, it is difficult to discern a clear trend on the results between KOH and KHCO₃. Originally, it was expected that the higher concentration of H⁺ present on more acidic anolytes paired with CEM would be able to regulate the pH more effectively near the cathode's surface and promote the CO₂RR. But contrary to what was expected, the CEM/CH₃COOH combination completely inhibits CO₂RR and exclusively produces H₂, while the CEM/KHCO₃ shows similar behaviour to CEM/KOH. The complete inhibition of CO₂RR in the CEM/CH₃COOH combination can be explained by an "over-acidification" of the pH near the cathode's surface, where an increase in the concentration of H⁺ leads to a shift of HER towards less negative potentials where CO₂RR is not a competitive reaction anymore. But it is uncertain what causes CEM/KHCO₃ and CEM/KOH to show similar behaviour, since it is expected that a slightly more acid anolyte like KHCO₃ should be able to provide H⁺ to the cathode in the same way a BPM does, and which result in favored CO₂RR. One possible explanation might be that there is an unknown mechanism which BPMs use to promote CO₂RR over HER other than the production of H⁺ towards the cathode.

Higher temperatures enhance FE_{CO}, particularly at higher current densities regardless of the membrane/anolyte combination. At a temperature of 50 °C the FE is even higher at a current density of 200 mA cm⁻² than at 100 mA cm⁻² with a temperature of 20 °C. Even though higher temperatures favor both HER and CO₂RR, it seems the effect is more pronounced in the latter. This is attributed to an increase in diffusion coefficients of CO₂ and HCO₃⁻, as well as more favorable thermodynamics and kinetics of the reaction [24]. Also, higher temperature favors CO₂ extraction and HCO₃⁻ dissociation which increases the supply and availability of CO₂ near the cathode's surface. Increasing the temperature beyond 50 °C has proven to increase the FE_{CO} further in

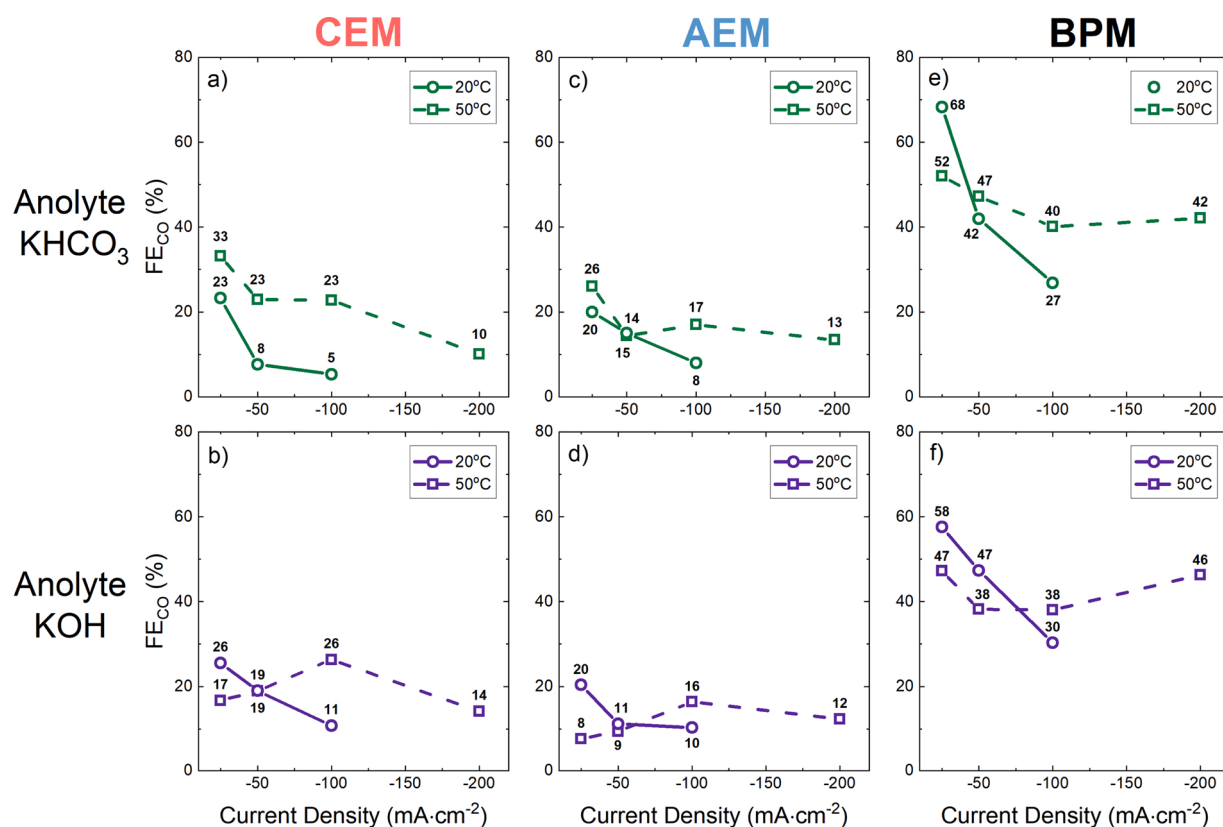


Fig. 4. Faradaic efficiency towards CO with different membranes, anolytes, and temperature.

CO₂RR systems with a concentrated bicarbonate feed [24], but higher temperatures also promote the release of gaseous CO₂ from the electrolyte which leads to a higher CO₂ concentration in the output, as will be discussed later.

3.2. Effect on cell potential

The polarity of the membrane greatly affects the cell potential, with AEM showing the best performance (Fig. 5) due to a higher availability of OH⁻ in both sides of the MEA which enables an effective exchange of ions across the membrane. The CEM improves its performance with KHCO₃ due to the higher number of protons in the anolyte, that can transport charge more rapidly than K⁺. On the other hand, the BPM's enhanced FE_{CO} comes with an important drawback in the form of an increase in cell potential (~1 V higher than AEM at 100 mA cm⁻²) since this type of membrane requires an additional potential to dissociate water molecules [29].

The anolyte's effect on the cell potential was as expected: a higher pH on the anolyte favors the OER which leads to decrease in cell potential. These results indicate that it is possible to use a highly alkaline solution on the anolyte without affecting the CO₂RR and contributing to a lower cell potential if OER is desired oxidation reaction. However, it is still undetermined if a highly alkaline solution (e.g. 1 M KOH) in the anode could be a potential issue to the chemical or mechanical stability of the MEA in long-term operation due to the corrosive nature of the solution.

An increase in temperature contributes to a decrease in cell potential due to more favorable thermodynamics for CO₂RR, HER and OER. The effect is even bigger in the CEM/KOH combination where the potential decreases by 750 mV at 100 mA cm⁻² compared to 280 mV and 420 mV of AEM and BPM, respectively. Even if raising the temperature from 20 °C to 50 °C represents an additional energy input to the system, some of this extra thermal energy is offset by a decrease in cell potential which represents a lower consumption of electrical energy.

3.3. Effect on residual CO₂

The residual CO₂ was calculated as the number of moles CO₂ collected in the phase separator divided by the total number of moles of gaseous products collected. It is important to point out that during all experiments, no gaseous CO₂ is formed in the bicarbonate solution before it enters the cell; all the gaseous CO₂ collected was produced inside the cell while current was being applied. It was discarded that the turbulence produced by the flow of the electrolyte through the flow-plate's serpentine is the cause of the release of CO₂ since no gas was accumulated when no current was applied to the cell. It is believed that gaseous CO₂ is formed inside the cell due to coulombic heating of the electrode caused by the flow of current [30] leading to a higher local temperature near the cathode which promotes the release of some of the dissolved CO₂ into gas. At higher current densities, the proportion of CO₂ becomes lower due to the faster rate of CO and H₂ production.

The membrane's polarity effect on residual CO₂ is maintained within 10–15 % difference between the three types tested (Fig. 6). Use of bipolar membrane results in higher residual CO₂, most likely due to its ability to produce extra CO₂ from the reaction between the generated H⁺ and the HCO₃⁻ in the catholyte.

The anolyte also affects the residual CO₂ but to a lesser extent. The systems with KHCO₃ solution in the anolyte resulted in 5–10 % higher CO₂ most likely to a higher probability of H⁺ species crossing the membrane and reacting with HCO₃⁻ to produce more CO₂ than the systems with KOH in the anolyte.

A rise in temperature increases the residual CO₂. Higher temperatures favor the dissociation of HCO₃⁻ to CO₂ which is favorable for the CO₂RR, but they also lower the solubility limit for CO₂ in water making it easier for the molecule to go from its dissolved phase to gaseous.

It is important to point out that for most of the conditions tested -and specially at higher current densities-, the residual CO₂ stays well below the 60–95 % range which systems with gaseous CO₂ feed produce.

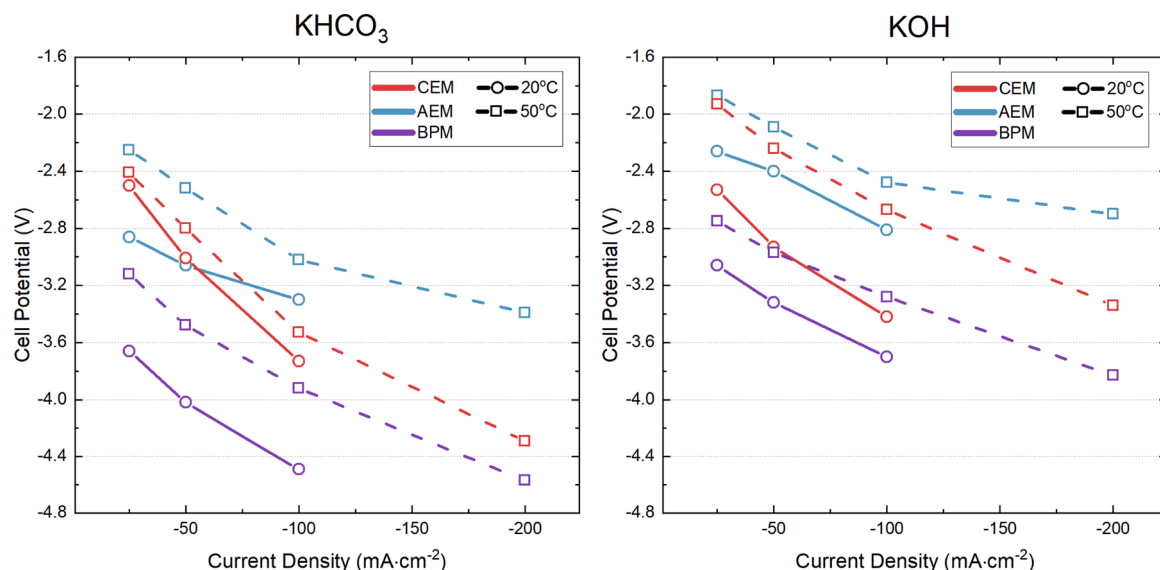


Fig. 5. Cell potential with different membranes and with KHCO_3 or KOH on the anolyte.

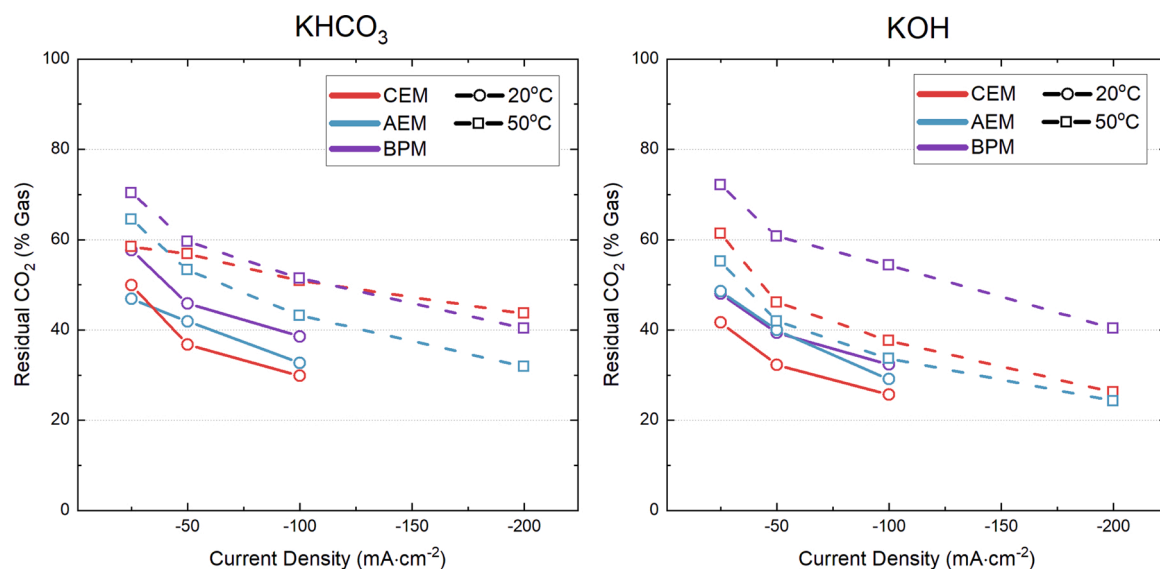


Fig. 6. Percentage of residual CO_2 accumulated in the output gas mixture with KHCO_3 or KOH as the anolyte.

Table 1
Characteristics and performance of state-of-art CO_2 electrolyzers.

Feedstock	Catalyst	Membrane	J (mA cm^{-2})	FE_{CO}	Reference
2 M KHCO_3	Ag	BPM	200	46 %	This work
3M KHCO_3	Ag	BPM	200	62 %	[31]
1 M K_2CO_3	Ag	BPM	200	20 %	[19]
CO_2 (g)	CoPc	AEM	200	88 %	[32]
CO_2 (g)	Ag	AEM	200	>90 %	[33]
CO_2 (g)	Ag	CEM	150	65 %	[34]
CO_2 (g)	Ag	–	417	100 %	[17]

Although there is still more effort needed for the CO_2RR systems with concentrated (bi)carbonate aqueous feed to reach the FE_{CO} and cell potentials achieved by systems with gaseous CO_2 feed (Table 1), the significant decrease in residual CO_2 upholds a promising prospect for this type of systems.

4. Conclusions

In this paper, the effect of the membrane's polarity, anolyte's solution, and operating temperature on CO_2RR systems with concentrated bicarbonate feedstock was studied. Particularly, their influence on faradaic efficiency, cell potential and residual CO_2 was investigated. It was determined that bipolar membranes significantly increase selectivity, with the important drawback of an increased cell potential. Higher temperatures also favor the evolution of CO over H_2 , while decreasing the overall cell potential. The anolyte does not impact the cathode's selectivity if the pH stays within an alkaline range, and a higher pH value leads to a lower cell potential since it promotes the OER. The use of concentrate bicarbonate as a CO_2 feedstock has the advantage of accumulating way less CO_2 in the output gas mixture than system that operate with a gaseous CO_2 feed.

Data availability

No data was used for the research described in the article.

CRediT authorship contribution statement

Carlos Larrea: Conceptualization, Methodology, Software, Validation, Formal analysis, Investigation, Resources, Data curation, Writing - original draft, Visualization. **Daniel Torres:** Methodology, Investigation, Resources. **Juan Ramón Avilés-Moreno:** Methodology, Resources, Writing - review & editing, Supervision. **Pilar Ocón:** Formal analysis, Resources, Writing - review & editing, Supervision, Project administration, Funding acquisition.

Declaration of Competing Interest

The authors declare that they have no known competing financial interests or personal relationships that could have appeared to influence the work reported in this paper.

Acknowledgements

This work was supported by the Madrid Regional Research Council (CAM) grant n. P2018/EMT-4344 BIOTRES-CM.

References

- [1] IPCC, *IPCC Fifth Assessment Report: Climate Change 2014*, Geneva, 2014.
- [2] D.A.N. Ussiri, R. Lal, Introduction to global carbon cycling: an overview of the global carbon cycle. *Carbon Sequestration Clim. Chang. Mitig. Adapt.*, Springer International Publishing, Cham, 2017, pp. 61–76, https://doi.org/10.1007/978-3-319-53845-7_3.
- [3] J. Hansen, P. Kharecha, M. Sato, V. Masson-Delmotte, F. Ackerman, D.J. Beerling, P.J. Hearty, O. Hoegh-Guldberg, S.-L. Hsu, C. Parmesan, J. Rockstrom, E. J. Rohling, J. Sachs, P. Smith, K. Steffen, L. Van Susteren, K. von Schuckmann, J. C. Zachos, Assessing “Dangerous climate change”: required reduction of carbon emissions to protect young people, future generations and nature, *PLoS One* 8 (2013) 1–26, <https://doi.org/10.1371/journal.pone.0081648>.
- [4] F.M. Baena-Moreno, M. Rodríguez-Galán, F. Vega, B. Alonso-Fariñas, L.F. V. Arenas, B. Navarrete, Carbon capture and utilization technologies: a literature review and recent advances, *Energy Sources, Part A Recover. Util. Environ. Eff.* 41 (2019) 1403–1433, <https://doi.org/10.1080/15567036.2018.1548518>.
- [5] A.A. Tountas, X. Peng, A.V. Tavasoli, P.N. Duchesne, T.L. Dingle, Y. Dong, L. Hurtado, A. Mohan, W. Sun, U. Ulmer, L. Wang, T.E. Wood, C.T. Maravelias, M. M. Sain, G.A. Ozin, Towards solar methanol: past, present, and future, *Adv. Sci.* 6 (2019), 1801903, <https://doi.org/10.1002/adv.201801903>.
- [6] M. Samavati, M. Santarelli, A. Martin, V. Nemanova, Production of synthetic Fischer–Tropsch diesel from renewables: thermoeconomic and environmental analysis, *Energy Fuels* 32 (2018) 1744–1753, <https://doi.org/10.1021/acs.energyfuels.7b02465>.
- [7] Y. Hori, Electrochemical CO₂ reduction on metal electrodes, in: C.G. Vayenas, R. E. White, M.E. Gamboa-Aldeco (Eds.), *Mod. Asp. Electrochem.*, Springer, New York, New York, NY, 2008, pp. 89–189, https://doi.org/10.1007/978-0-387-49489-0_3.
- [8] A. de Klerk, Fischer–Tropsch process. *Kirk-Othmer Encycl. Chem. Technol.*, American Cancer Society, 2013, pp. 1–20, <https://doi.org/10.1002/0471238961.fiscdekl.a01>.
- [9] C. Xiang, K.M. Papadantonakis, N.S. Lewis, Principles and implementations of electrolysis systems for water splitting, *Mater. Horiz.* 3 (2016) 169–173, <https://doi.org/10.1039/C6MH00016A>.
- [10] R.I. Masel, Z. Liu, H. Yang, J.J. Kaczur, D. Carrillo, S. Ren, D. Salvatore, C. P. Berlinguette, An industrial perspective on catalysts for low-temperature CO₂ electrolysis, *Nat. Nanotechnol.* (2021), <https://doi.org/10.1038/s41565-020-00823-x>.
- [11] D. Salvatore, C.P. Berlinguette, Voltage matters when reducing CO₂ in an electrochemical flow cell, *ACS Energy Lett.* 5 (2020) 215–220, <https://doi.org/10.1021/acsenrgylett.9b02356>.
- [12] J. Herranz, A. Pátru, E. Fabbri, T.J. Schmidt, Co-electrolysis of CO₂ and H₂O: from electrode reactions to cell-level development, *Curr. Opin. Electrochem.* 23 (2020) 89–95, <https://doi.org/10.1016/j.coelec.2020.05.004>.
- [13] R. Krause, D. Reinisch, C. Reller, H. Eckert, D. Hartmann, D. Taroata, K. Wiesner-Fleischer, A. Bulan, A. Lueken, G. Schmid, Industrial application aspects of the electrochemical reduction of CO₂ to CO in aqueous electrolyte, *Chemie Ing. Tech.* 92 (2020) 53–61, <https://doi.org/10.1002/cite.201900092>.
- [14] A.J. Martín, G.O. Larrazábal, J. Pérez-Ramírez, Towards sustainable fuels and chemicals through the electrochemical reduction of CO₂: lessons from water electrolysis, *Green Chem.* 17 (2015) 5114–5130, <https://doi.org/10.1039/C5GC01893E>.
- [15] S. Verma, X. Lu, S. Ma, R.I. Masel, P.J.A. Kenis, The effect of electrolyte composition on the electroreduction of CO₂ to CO on Ag based gas diffusion electrodes, *Phys. Chem. Chem. Phys.* 18 (2016) 7075–7084, <https://doi.org/10.1039/C5CP05665A>.
- [16] C.-T. Dinh, F.P. García de Arquer, D. Sinton, E.H. Sargent, High rate, selective, and stable electroreduction of CO₂ to CO in basic and neutral media, *ACS Energy Lett.* 3 (2018) 2835–2840, <https://doi.org/10.1021/acsenrgylett.8b01734>.
- [17] S.S. Bhargava, F. Proietto, D. Azmoodeh, E.R. Cofell, D.A. Henckel, S. Verma, C. J. Brooks, A.A. Gewirth, P.J.A. Kenis, System design rules for intensifying the electrochemical reduction of CO₂ to CO on Ag nanoparticles, *ChemElectroChem.* 7 (2020) 2001–2011, <https://doi.org/10.1002/celec.202000089>.
- [18] A.J. Welch, E. Dunn, J.S. DuChene, H.A. Atwater, Bicarbonate or carbonate processes for coupling carbon dioxide capture and electrochemical conversion, *ACS Energy Lett.* 5 (2020) 940–945, <https://doi.org/10.1021/acsenrgylett.0c00234>.
- [19] Y.C. Li, G. Lee, T. Yuan, Y. Wang, D.-H. Nam, Z. Wang, F.P. de Arquer, Y. Lum, C.-T. Dinh, O. Voznyy, E.H. Sargent, CO₂ electroreduction from carbonate electrolyte, *ACS Energy Lett.* 4 (2019) 1427–1431, <https://doi.org/10.1021/acsenrgylett.9b00975>.
- [20] T. Li, E.W. Lees, M. Goldman, D.A. Salvatore, D.M. Weekes, C.P. Berlinguette, Electrolytic conversion of bicarbonate into CO in a flow cell, *Joule* 3 (2019) 1487–1497, <https://doi.org/10.1016/j.joule.2019.05.021>.
- [21] D.W. Keith, G. Holmes, D. St. Angelo, K. Heidel, A process for capturing CO₂ from the atmosphere, *Joule* 2 (2018) 1573–1594, <https://doi.org/10.1016/j.joule.2018.05.006>.
- [22] K. Teramura, K. Hori, Y. Terao, Z. Huang, S. Iguchi, Z. Wang, H. Asakura, S. Hosokawa, T. Tanaka, Which is an intermediate species for photocatalytic conversion of CO₂ by H₂O as the electron donor: CO₂ molecule, carbonic acid, bicarbonate, or carbonate ions? *J. Phys. Chem. C* 121 (2017) 8711–8721, <https://doi.org/10.1021/acs.jpcc.6b12809>.
- [23] M. Dunwell, Q. Lu, J.M. Heyes, J. Rosen, J.G. Chen, Y. Yan, F. Jiao, B. Xu, The central role of bicarbonate in the electrochemical reduction of carbon dioxide on gold, *J. Am. Chem. Soc.* 139 (2017) 3774–3783, <https://doi.org/10.1021/jacs.6b13287>.
- [24] Z. Zhang, L. Melo, R.P. Janssonius, F. Habibzadeh, E.R. Grant, C.P. Berlinguette, pH matters when reducing CO₂ in an electrochemical flow cell, *ACS Energy Lett.* 5 (2020) 3101–3107, <https://doi.org/10.1021/acsenrgylett.0c01606>.
- [25] D.A. Salvatore, D.M. Weekes, J. He, K.E. Dettelbach, Y.C. Li, T.E. Mallouk, C. P. Berlinguette, Electrolysis of gaseous CO₂ to CO in a flow cell with a bipolar membrane, *ACS Energy Lett.* 3 (2018) 149–154, <https://doi.org/10.1021/acsenrgylett.7b01017>.
- [26] M.R. Singh, Y. Kwon, Y. Lum, J.W. Ager, A.T. Bell, Hydrolysis of electrolyte cations enhances the electrochemical reduction of CO₂ over Ag and Cu, *J. Am. Chem. Soc.* 138 (2016) 13006–13012, <https://doi.org/10.1021/jacs.6b07612>.
- [27] A. Wuttig, Y. Surendranath, Impurity ion complexation enhances carbon dioxide reduction catalysis, *ACS Catal.* 5 (2015) 4479–4484, <https://doi.org/10.1021/acscatal.5b00808>.
- [28] Y.C. Li, Z. Yan, J. Hitt, R. Wycisk, P.N. Pintauro, T.E. Mallouk, Bipolar membranes inhibit product crossover in CO₂ electrolysis cells, *Adv. Sustain. Syst.* 2 (2018), 1700187, <https://doi.org/10.1002/adsu.201700187>.
- [29] R.S. Reiter, W. White, S. Ardo, Electrochemical characterization of commercial bipolar membranes under electrolyte conditions relevant to solar fuels technologies, *J. Electrochem. Soc.* 163 (2015) H3132–H3134, <https://doi.org/10.1149/2.0201604jes>.
- [30] A.Q. Fenwick, O.R. Luca, The formation of CO by thermal decomposition of formic acid under electrochemical conditions of CO₂ reduction, *J. Photochem. Photobiol. B, Biol.* 152 (2015) 43–46, <https://doi.org/10.1016/j.jphotobiol.2015.04.003>.
- [31] E.W. Lees, M. Goldman, A.G. Fink, D.J. Dvorak, D.A. Salvatore, Z. Zhang, N.W. X. Loo, C.P. Berlinguette, Electrodes designed for converting bicarbonate into CO, *ACS Energy Lett.* 5 (2020) 2165–2173, <https://doi.org/10.1021/acsenrgylett.0c00898>.
- [32] S. Ren, D. Joulié, D. Salvatore, K. Torbensen, M. Wang, M. Robert, C. P. Berlinguette, Molecular electrocatalysts can mediate fast, selective CO₂ reduction in a flow cell, *Science* (80-) 365 (2019) 367–369, <https://doi.org/10.1126/science.aax4608>.
- [33] R.B. Kutz, Q. Chen, H. Yang, S.D. Sajjad, Z. Liu, I.R. Masel, Sustainion imidazolium-functionalized polymers for carbon dioxide electrolysis, *Energy Technol.* 5 (2017) 929–936, <https://doi.org/10.1002/ente.201600636>.
- [34] P. Jeanty, C. Scherer, E. Magori, K. Wiesner-Fleischer, O. Hinrichsen, M. Fleischer, Upscaling and continuous operation of electrochemical CO₂ to CO conversion in aqueous solutions on silver gas diffusion electrodes, *J. CO₂ Util.* 24 (2018) 454–462, <https://doi.org/10.1016/j.jcou.2018.01.011>.